

## Fascinating Diazirinone: A Violet Gas

Xiaoqing Zeng,<sup>\*[a]</sup> Helmut Beckers,<sup>[a]</sup> Helge Willner,<sup>[a]</sup> and John F. Stanton<sup>\*[b]</sup>

**Keywords:** Small ring systems / Matrix isolation / IR spectroscopy / Raman spectroscopy / UV/Vis spectroscopy / Electronic structure / Ab initio calculations

Diazirinone (cyclic N<sub>2</sub>CO) recently identified in solid noble gas matrices and in the gas phase by infrared spectroscopy, has now been trapped at -196 °C as a neat brownish-yellow solid, and characterized by low-temperature IR and Raman spectroscopy. Evaporation of the solid yields violet gaseous N<sub>2</sub>CO, which is surprisingly stable in a clean quartz cell. Its decay at room temperature in the dark follows a second-order rate law ( $k_2 = 4.9 \times 10^{-2} \text{ L mol}^{-1} \text{ s}^{-1}$ ) with a half-life of 30 h at an initial pressure of 5 mbar. The visible absorption spec-

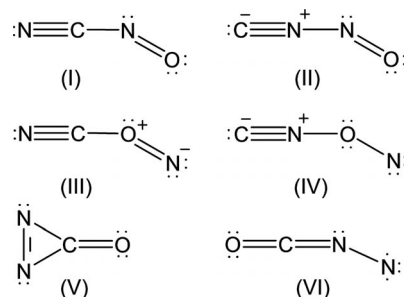
trum of the gas reveals a structured band with the 0–0 transition at 567 nm (17651 cm<sup>-1</sup>), and its assignment has been made with the aid of theoretical calculations. Cyclic diazirinone that is isolated in solid Ar at 16 K decomposes upon visible light irradiation to yield N<sub>2</sub> and CO, but after being exposed to ArF excimer laser irradiation (193 nm) the N=N bond is cleaved and the open-chain isomers NOCN, ONCN, and ONNC are formed.

### Introduction

The isoelectronic molecules N<sub>2</sub>CO,<sup>[1]</sup> N<sub>4</sub>,<sup>[2]</sup> and C<sub>2</sub>O<sub>2</sub><sup>[3]</sup> are high-energy dimers of the strongest bonded diatomic molecules N<sub>2</sub> and CO. They are of fundamental interest, and much effort has been spent in searching for them. Their spectroscopic and structural properties, chemistry, as well as their possible formation in the atmosphere or in interstellar clouds, have been explored by theoretical studies.<sup>[1–3]</sup> Experimental approaches to these metastable species are strongly hampered by the lack of suitable synthetic strategies, e.g., neither N<sub>4</sub> nor C<sub>2</sub>O<sub>2</sub> has been isolated, although N<sub>4</sub> has been detected by means of neutralization/reionization mass spectrometry (NRMS), where a short lifetime of about 1 μs at 298 K in the gas phase was estimated for the most likely open-chain geometry.<sup>[2]</sup>

Among the [N<sub>2</sub>,C,O] species (Scheme 1), nitrosyl cyanide, ONCN (**I**) is well known and easily accessible from AgCN and ClNO.<sup>[4]</sup> Another two open-chain isomers, nitrosyl isocyanide (ONNC, **II**) and isonitrosyl cyanide (NOCN, **III**), have been obtained in solid noble gas matrices by photoisomerization of ONCN.<sup>[5]</sup> For carbonyl isodiazenes (OCNN, **VI**), theoretical calculations predict a triplet ground state, the singlet species is not a minimum on the potential energy surface. In an NRMS experiment com-

bined with quantum chemical calculations the detection of the triplet species was claimed and its lifetime estimated to be ca. 0.8 μs.<sup>[6]</sup> According to previous calculations,<sup>[1a]</sup> the most stable isomer on the singlet potential energy surface is the diazirinone (cyclic N<sub>2</sub>CO, **V**). A significant barrier of 108 kJ mol<sup>-1</sup>, resulting from aromatic stabilization, was predicted for its exothermic (400 kJ mol<sup>-1</sup>) dissociation into N<sub>2</sub> and CO.



Scheme 1. Six isomers with a composition of [N<sub>2</sub>,C,O].

A straightforward synthetic approach to this cyclic isomer is still missing. It was first suggested to be formed by the elimination of 1-fluoro-4-nitrobenzene from 3-chloro-3-(4-nitrophenoxy)diazirine in the presence of fluoride, but the transient IR band at 2150 cm<sup>-1</sup>, produced in these experiments and erroneously assigned to **V**,<sup>[7,8]</sup> was later attributed to its decomposition product CO in the condensed phase.<sup>[9]</sup> More recently, **V** has been identified in solid noble gas matrices as an unanticipated pyrolysis product of OC(N<sub>3</sub>)<sub>2</sub>.<sup>[10]</sup> A subsequent low-pressure pyrolysis of OC(N<sub>3</sub>)<sub>2</sub> yielded **V**, which allowed the IR gas-phase measurements at high resolution.<sup>[11]</sup> Experimental ground-state rotational constants of **V** were estimated from an analysis

[a] Bergische Universität Wuppertal, FB C – Mathematik und Naturwissenschaften – Fachgruppe Chemie  
42119 Wuppertal, Germany  
Fax: +49-202-439-3053  
E-mail: zeng@uni-wuppertal.de

[b] University of Texas  
1 University Station A5300, Austin, 78712-0165 Texas, USA  
E-mail: jfstanton@mail.utexas.edu

Supporting information for this article is available on the WWW under <http://dx.doi.org/10.1002/ejic.201200337>.

of the strong Fermi couple  $\nu_1$  and  $2\nu_5$ .<sup>[11]</sup> More recently the formation of **V** has been claimed under irradiation of a 60 keV Ar<sup>2+</sup> ion beam on CO/N<sub>2</sub> ices at 10 K.<sup>[12]</sup>

As pointed out by a recent highlight,<sup>[13]</sup> the knowledge of the general physical and spectroscopic properties for such a fundamental species is desirable. Herein we report the preparation and thermal decay of pure **V**, its characterization in the solid (IR and Raman spectroscopy) and gaseous states (UV/Vis spectroscopy), and its photochemistry in solid Ar matrices.

## Results and Discussion

### Improved Synthesis of OC(N<sub>3</sub>)<sub>2</sub> and Cyclic N<sub>2</sub>CO (**V**)

For the synthesis of diazirinone,<sup>[10]</sup> pure carbonyl diazide [OC(N<sub>3</sub>)<sub>2</sub>] is used as a precursor. In the previously reported synthesis of OC(N<sub>3</sub>)<sub>2</sub>,<sup>[14]</sup> the reaction of NaN<sub>3</sub> and FC(O)Cl (in excess) was performed in flame-sealed glass ampules at room temperature for 4 d, followed by cutting the ampules and separating the volatile mixture in a vacuum line. The monoazide FC(O)N<sub>3</sub> was obtained as the main product. However, cutting glass ampules containing such highly explosive carbonyl diazide by using the ampule-key technique<sup>[15]</sup> can lead to explosions. In addition, when the reaction mixture was cooled prior to cutting the ampules, heavy explosions were also occasionally encountered, especially when an excess of NaN<sub>3</sub> was used. However, no explosion was experienced when a pure liquid OC(N<sub>3</sub>)<sub>2</sub> sample was solidified by using liquid nitrogen, or rapidly warmed to room temperature.

In this work, the synthesis of OC(N<sub>3</sub>)<sub>2</sub> was performed in two steps by using common tube-like glass vessels (volume 25 mL, length 20 cm) equipped with a valve fitted with a PTFE stem (Young, London, UK). First, the monoazide, FC(O)N<sub>3</sub>, was synthesized by using NaN<sub>3</sub> and an excess of FC(O)Cl. Then, purified FC(O)N<sub>3</sub> was treated with equimolar NaN<sub>3</sub> at room temperature for 3 d. The vessel was very slowly opened at the vacuum line, and the volatile products were separated by passing through cold traps kept at -60 and -196 °C. The product OC(N<sub>3</sub>)<sub>2</sub> was retained in nearly quantitative yield as a white solid at -60 °C and was used for the vacuum-pyrolysis experiments without further purification. About 120 mg of OC(N<sub>3</sub>)<sub>2</sub> was prepared in two batches.

The low-pressure pyrolysis of OC(N<sub>3</sub>)<sub>2</sub> was performed at about 420 °C. As an improvement to the previous pyrolysis experiment,<sup>[10]</sup> a quartz rather than a glass tube, equipped with some quartz wool inside, was used and found to increase the yield of **V**. The decomposition of the diazide was monitored by the pressure of the noncondensable gases passing the two successive cold traps kept at -110 and -196 °C. Some diazide was recovered in the first trap and used for further pyrolysis experiments. In the second trap a yellow solid was obtained, which was purified by repeated fractional condensation of the vapor at low temperatures. The vapor-phase IR spectrum of the pure product revealed the two strong bands at 2044 ( $\nu_1$ ) and 1865 cm<sup>-1</sup> ( $2\nu_5$ ), pre-

viously attributed to **V**.<sup>[10]</sup> Eventually, the brownish-yellow solid (about 5 mg) was obtained in the -145 °C trap from the pyrolysis of OC(N<sub>3</sub>)<sub>2</sub> (120 mg). Some decomposition of the gaseous product in the glass vacuum line was evidenced by the formation of noncondensable gases (N<sub>2</sub> + CO).

Solid diazirinone can be stored in sealed glass ampules at liquid nitrogen temperatures for several weeks without apparent decomposition. The thermal decay of gaseous **V** into N<sub>2</sub> + CO depends strongly on the material of the container. In stainless steel vessels, **V** decomposes within minutes and in an IR glass cell fitted with Si windows the decay follows a first-order rate law with a half-life at 21 °C of 1.4 h (Figure S1 in the Supporting Information).<sup>[10]</sup> In a dry quartz UV cell the depletion follows an unexpected second-order rate with a half-life of 30 h at an initial pressure of 5 mbar and a temperature of 20 °C. The rate constant was determined to be  $k_2 = 4.9 \times 10^{-2} \text{ L mol}^{-1} \text{ s}^{-1}$  (Figures S2 and S3 in the Supporting Information). These observations indicate strong surface-catalyzed thermal decomposition of **V** in stainless steel or glass vessels, but the detailed mechanism remains unknown.

### Vibrational Spectroscopy of Cyclic N<sub>2</sub>CO (**V**)

Gaseous **V**, highly diluted in argon (ca. 1:1000), was deposited as a matrix at 16 K. Its IR spectrum is shown in Figure 1 (upper trace). The band positions and relative intensities are identical with those of the previously reported spectrum of **V** obtained from matrix-isolated thermal decomposition products of OC(N<sub>3</sub>)<sub>2</sub>.<sup>[10]</sup> In addition, traces of CO, CO<sub>2</sub>, HNCO, and H<sub>2</sub>O were identified in the spectrum. The IR spectrum of pure solid N<sub>2</sub>CO (Figure 1, middle trace) was recorded after gaseous **V** was deposited on a thin film of solid Ne at 6 K.

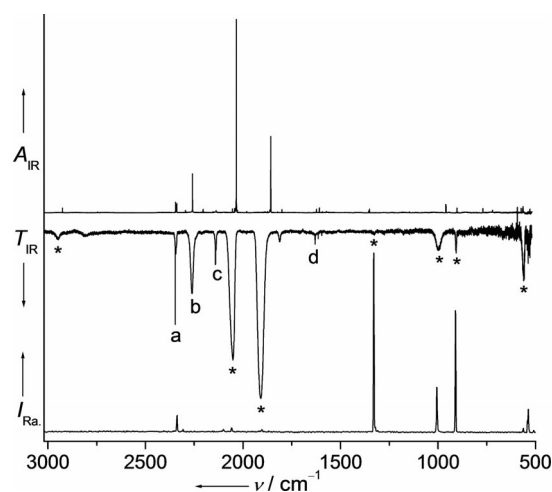


Figure 1. Upper trace: IR spectrum of Ar-matrix-isolated diazirinone (**V**) (absorption  $A$ , 16 K, res. 0.25 cm<sup>-1</sup>). Middle trace: IR spectrum of solid **V** (transmission  $T$ , 6 K, res. 2 cm<sup>-1</sup>). Lower trace: Raman spectrum of solid **V** (Raman intensity  $I$ , 77 K, res. 2 cm<sup>-1</sup>). Bands of **V** (\*), CO<sub>2</sub> (a), HNCO (b), CO (c), and H<sub>2</sub>O (d) are labeled.

Compared to the IR spectrum of matrix-isolated **V**, the IR bands of the neat solid are strikingly broadened and

Table 1. Calculated and observed vibrational frequencies ( $\text{cm}^{-1}$ ) of diazirirone (**V**).

Calculated <sup>[a]</sup>	IR <sup>[b]</sup>	IR <sup>[c]</sup>	IR	Raman <sup>[c]</sup>	Assignment
	Ar matrix (16 K)	Solid (6 K)		Gas phase (298 K)	
2939(7.0)	2925.2(1)	2951 vw			$a_1$ $\nu_1 + \nu_3$
2046(316.7)	2033.6(100)	1909 vs	2043.8 <sup>[d]</sup>	1904 vw	$\nu_1$ , C=O stretch
1860(120.7)	1857.4(55)	2052 s	1863.3 <sup>[d]</sup>	2058 vw	$2\nu_5$
1325(0.2)			1331 <sup>[e]</sup>	1329 vs	$\nu_2$ , N=N stretch
903(5.2)	902.2(2)	907 w	904.5 <sup>[f]</sup>	911 s	$\nu_3$ , NCN s-stretch
565(28.7)	564.4(11)	560 m		564 w	$b_1$ $\nu_4$ , out-of-plane bend
961(11.3)	959.6(6)	1001 m	962 <sup>[f]</sup>	1007 m	$b_2$ $\nu_5$ , NCN as-stretch
529(11.9)	528.9(4)			537 m	$\nu_6$ , OCN rock

[a] Calculated [CCSD(T)/ANO2] anharmonic IR frequencies and intensities ( $\text{km mol}^{-1}$ ) in parentheses are taken from ref.<sup>[10]</sup> [b] Observed IR band positions and integrated relative intensities (in parentheses). [c] Relative intensities: vs. very strong, s strong, m medium, w weak, vw very weak. [d] Band positions of the Fermi couple,  $\nu_1$  and  $2\nu_5$ , were taken from ref.<sup>[11]</sup> [e] Frequency derived from a hot band in the electronic spectrum of gaseous **V** (see below). [f] Band origin estimated from gas-phase IR spectrum at  $2\text{ cm}^{-1}$  resolution.

shifted, particularly for the two strongest bands at 1909 and  $2052\text{ cm}^{-1}$  (Ar matrix: 1857.4 and  $2033.6\text{ cm}^{-1}$ ; gas phase: 1863.3 and  $2043.8\text{ cm}^{-1}$ ). In the gas-phase and Ar-matrix spectra these bands were assigned to the Fermi couple  $\nu_1$  and  $2\nu_5$ . The higher energy feature is stronger in intensity and therefore is described as the  $\nu_1$  fundamental. However, while the stronger band appeared in the matrix spectrum at a higher energy, the situation is reversed in the spectrum of the solid. This profound change is due to intermolecular interactions in the solid, so that the level associated with the overtone rises above that of the fundamental, which results in the observed change in intensity. Consistent with this observation is the blueshift of more than  $40\text{ cm}^{-1}$  for the asymmetric N–C–N stretching band  $\nu_5$  in the solid state ( $1001\text{ cm}^{-1}$ ) compared to that of the matrix-isolated molecules ( $959.6\text{ cm}^{-1}$ ), which – in the absence of a corresponding shift of the CO stretching mode – is sufficiently large to account for the observed phenomenon.

The assignments of the IR bands to the Fermi-coupled pair of states  $\nu_1$  and  $2\nu_5$  are in excellent agreement with a deperturbation treatment of the interaction at the CCSD(T) level by using the ANO2 basis set.<sup>[10]</sup> The deperturbed levels from theory are 2005 and  $1901\text{ cm}^{-1}$  for  $\nu_1$  and  $2\nu_5$ , respectively. The experimental frequencies have also been corrected for the Fermi resonance induced frequency shifts<sup>[16]</sup> (Table S1 in the Supporting Information). The excellent agreement between the deperturbed values for  $2\nu_5$  with those of  $2 \times \nu_5$  (Table S1 in the Supporting Information) strongly supports the assignment of these bands (Table 1). Intermolecular interactions may also account for the large solid-state broadening of the  $\nu_5$  and  $2\nu_5$  bands in the disordered amorphous solid. The solid-state shift of the asymmetric NCN stretching frequency further reveals a substantial strengthening of the C–N bond in the solid state compared to that in the gas phase. Thus, the two fragments CO and  $\text{N}_2$  seem to be more strongly bonded in the solid state.

The Raman spectrum of the solid at  $-196\text{ }^\circ\text{C}$  is also shown in Figure 1 (lower trace). The Raman bands for  $\nu_1$  and  $2\nu_5$  occur as very weak features at 1904 and  $2058\text{ cm}^{-1}$ , respectively, while the fundamentals  $\nu_3$  and  $\nu_5$  appear as sharp bands at 911 and  $1007\text{ cm}^{-1}$ , respectively. All Raman-band positions are quite close to those observed in the IR

spectrum of the solid (Table 1). The strongest Raman band at  $1329\text{ cm}^{-1}$  is assigned to the N–N stretching vibration ( $\nu_2$ ). This band has not been observed in the IR spectra, but its frequency has been estimated from a hot band in the electronic spectrum of gaseous **V** (see below) at  $1331\text{ cm}^{-1}$ .

### Electronic Spectrum of Cyclic $\text{N}_2\text{CO}$ (**V**)

Upon evaporation of solid **V** its color changes from a brownish-yellow solid to a violet gas. The visible absorption spectrum of the gas reveals a structured band with a 0–0 transition at 567 nm ( $17651\text{ cm}^{-1}$ ; Figure 2). The electronic spectrum of **V** isolated in an Ne matrix at 6 K (Figure S4 in the Supporting Information) shows no hot bands but a very similar vibrational profile.

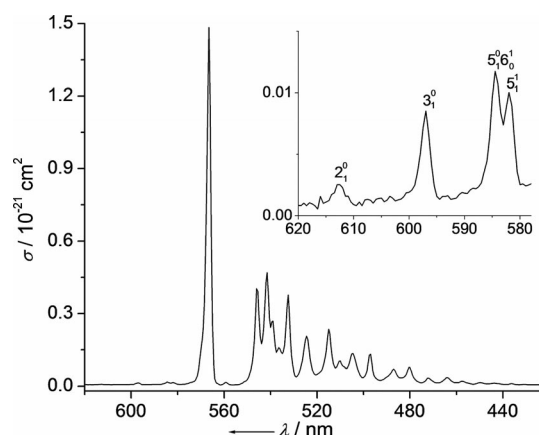


Figure 2. The visible absorption spectrum of gaseous **V** (quartz cell, 298 K, length 5 cm). Inset: enlarged spectrum in the region of 620–578 nm with vibronic hot bands.

The calculated structural parameters compiled in Table 2 predict the three-membered ring of **V** in the ground state to be retained in the excited state, where the N–N bond is significantly elongated from 132.4 pm in the  $X^1A_1$  ground state to 141.2 pm in the  $A^1B_1$  excited state at the CCSD(T)/ANO1 level of theory. This lowest dipole-allowed transition ( $A^1B_1 \leftarrow X^1A_1$ ) is mainly attributed to a one-electron promotion from the highest occupied molecular orbital ( $b_2$ , HOMO) to the lowest unoccupied molecular orbital ( $a_2$ ,

Table 2. Calculated structures, adiabatic transition energies  $T_0$  (eV), and harmonic vibrational energies ( $\text{cm}^{-1}$ ) for the ground ( $X^1A_1$ ) and the first excited electronic state ( $A^1B_1$ ), as well as experimentally determined upper-state vibrational energies ( $\text{cm}^{-1}$ ) from the visible  $A^1B_1 \leftarrow X^1A_1$  transition of diazirinone (**V**).

Parameters <sup>[a]</sup>	$X^1A_1$			$A^1B_1$			Experimental
	CCSD ANO0	CCSD(T) ANO0	CCSD(T) ANO1	CCSD ANO0	CCSDT ANO0	CCSDT ANO1	
$R(\text{C-O})$	119.0	119.5	118.9	118.1	120.1	119.3	
$R(\text{C-N})$	138.7	139.8	138.7	138.6	138.6	138.0	
$R(\text{N-N})$	131.6	133.5	132.4	139.6	143.5	141.2	
$\angle(\text{NCN})$	56.6	57.1	57.0	60.4	62.4	61.5	
$T_0$	0.00	0.00	0.00	2.47	2.26	2.20	2.19
$\nu_1$	2085.5	2038.0	2043.5	1975.3	1761.4	1807.4	1770
$\nu_2$	1398.0	1298.4	1335.6	1225.3	1125.6	1160.8	1131
$\nu_3$	934.8	898.2	917.7	793.5	687.2	741.7	668
$\nu_4$	590.0	570.1	567.7	621.6	596.2	621.1	709 <sup>[b]</sup>
$\nu_5$	1029.6	974.2	983.5	542.1	619.8	589.9	493 <sup>[b]</sup>
$\nu_6$	547.9	530.6	535.01	413.8	442.1	437.7	418

[a] Calculated bond lengths in [pm] and angles in [°]. [b] Tentative.

LUMO). The HOMO can be described as an in-plane and out-of-phase combination of  $\sigma$ -type CN bonding and oxygen lone-pair orbitals (Figure 3 and Table S2 in the Supporting Information), and the LUMO is the antibonding  $\pi^*(\text{N}=\text{N})$  orbital. A related electronic transition is common to other diazirines, where it has been observed for  $\text{H}_2\text{CN}_2$  (0–0 transition at 320 nm)<sup>[17]</sup> and  $\text{F}_2\text{CN}_2$  (0–0: 393 nm).<sup>[18]</sup> It shifts to the visible region for gaseous **V** (0–0: 567 nm).

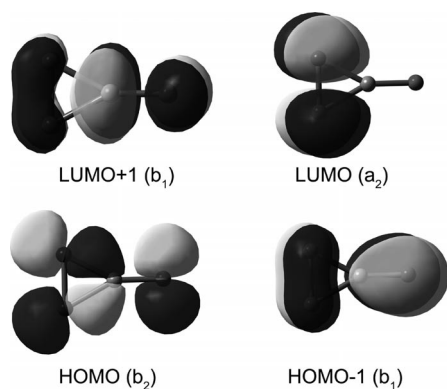


Figure 3. Frontier molecular orbital plots (isovalue = 0.04) of **V** calculated at the B3LYP/6-311+G(3df) level.

On the basis of the position of the peaks observed in the electronic spectrum (with respect to the unambiguous 0–0 transition, see Table S3 in the Supporting Information), an assignment that allows identification of upper-state vibrational frequencies has been made. They are listed in Table 2 and agree reasonably well with the harmonic frequencies calculated at the EOM-CCSDT/ANO1 level of theory. The totally symmetric fundamentals are easily assigned from the spectrum, and their positions can be considered secure. The two upper-state fundamentals, corresponding to the  $\nu_5$  (NCN asymmetric-stretching) and  $\nu_6$  (OCN rocking) fundamentals with  $b_2$  symmetry, were estimated from features that were assigned to hot bands and/or transitions to combination and overtone levels. Because of the possible effects of cross-anharmonicity and resonances, the positions of these two fundamental transitions

are somewhat uncertain. The assignments given in Table S3 in the Supporting Information can be regarded as tentative. Especially assignments corresponding to  $\nu_4$  require a more thorough study of the electronic spectrum, which should be an appropriate topic for further studies. In any event, it is clear from the assignments that at least most of the vibrational modes in the  $A^1B_1$  state have lower frequencies than the corresponding modes in the ground electronic state, and that this decrease is particularly large for the asymmetric C–N stretching mode  $\nu_5$ . These observations are comparable to those reported for other diazirines in the excited  $A^1B_1$  state.<sup>[19]</sup> The low asymmetric C–N stretching frequency was suggested to facilitate the decomposition of electronically excited diazirines through an asymmetric ring opening. In addition to the visible band, an unstructured band centered at around 200 nm was observed, which revealed a similar photolysis behavior as the visible band of **V** (Figure S5 in the Supporting Information), although other species such as HNCO and CO may contribute to this absorption.

A remarkable feature of the calculated structure of **V** is the rather long N=N bond lengths of 132.4 pm in the ground-state equilibrium structure. This value is intermediate between an N=N double bond length (120 pm) and an N–N single bond length (142 pm),<sup>[20]</sup> and also significantly longer than the N=N distances in the related diazirines,  $\text{H}_2\text{CN}_2$  [122.80(25) pm, microwave spectroscopy]<sup>[21]</sup> and  $\text{F}_2\text{CN}_2$  [129.3(9) pm, electron diffraction].<sup>[22]</sup> The marked decrease in the N=N bond lengths in the series  $\text{H}_2\text{CN}_2 < \text{F}_2\text{CN}_2 < \text{V}$  is, however, consistent with the expected variation in the hybridization of the carbon valence orbitals involved in the C–N bonds.<sup>[23]</sup> According to Bent's rule,<sup>[23]</sup> a widening of the N–C–N angles along this series,  $48.98(15)^\circ$  ( $\text{H}_2\text{CN}_2$ )<sup>[21]</sup>  $< 54.0(4)^\circ$  ( $\text{F}_2\text{CN}_2$ )<sup>[22]</sup>  $< 57.0^\circ$  (**V**), can be attributed to an increasing 2s-type character of the respective carbon hybrid orbitals.

#### Photochemistry of Cyclic $\text{N}_2\text{CO}$ (**V**)

The photodecomposition of **V** to  $\text{N}_2$  and CO under near-UV/Vis light irradiation ( $\lambda > 335$  nm) has previously been

reported.<sup>[10]</sup> Now, after its UV/Vis absorption spectrum is known, more selective irradiations can be applied. First, visible light irradiation of  $\lambda > 530$  nm was applied to the Ar-matrix-isolated sample, and simultaneously, the bands associated with diazirine strongly decreased, and only one new band at  $2140.0\text{ cm}^{-1}$  appeared in the IR spectrum. The carrier of the new band is Ar-matrix-isolated CO, indicating a photodestruction of **V** at these wavelengths to form  $\text{CO} + \text{N}_2$  (not IR-active).

When **V** was subjected to ArF excimer laser irradiation ( $\lambda = 193$  nm), the IR band of CO was also observed. However, in addition, a strong band from the NO stretching mode of the open-chain isomer, NO–CN (**III**), appeared at  $1837.0\text{ cm}^{-1}$ . The difference IR spectrum depicted in Figure 4 illustrates the spectral changes upon irradiation. Two additional weak bands at  $1681.1$  and  $1498.5\text{ cm}^{-1}$  in the product spectrum (pointing upwards) are assigned, according to previous Ar-matrix-isolation studies,<sup>[5]</sup> to the NO stretching modes of the valence isomers ON–NC (**II**) and ON–CN (**I**), respectively. As reported previously,<sup>[5]</sup> the mutual interconversion between the three chain isomers, **I**, **II**, and **III**, can be achieved by selective irradiations (Figure S6 in the Supporting Information).

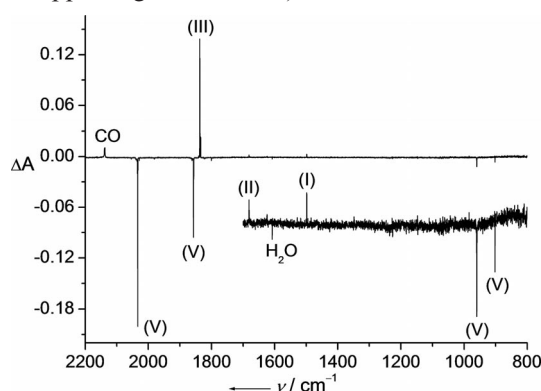


Figure 4. IR difference spectrum (absorption  $A$ , 16 K, res.  $0.25\text{ cm}^{-1}$ ) showing the spectral changes after ArF excimer laser photolysis ( $\lambda = 193$  nm) of Ar-matrix-isolated cyclic  $\text{N}_2\text{CO}$ . Bands of cyclic  $\text{N}_2\text{CO}$  (**V**) (pointing downward) and of ONCN (**I**), ONNC (**II**), NOCN (**III**), and CO (pointing upward) are indicated.

To the best of our knowledge, a photoinduced ring-opening of diazirines by  $\text{N}=\text{N}$  bond cleavage has not been reported so far. As mentioned above, **V** exhibits an absorption at about 200 nm (Figure S5 in the Supporting Information). The corresponding  $^1B_2$  excited state mainly derives from contributions of a one-electron promotion from the HOMO-1 ( $b_1$ , Figure 3) to the  $\pi^*(\text{NN})$  antibonding LUMO ( $a_2$ ).

The  $\text{CN}_2$  ring is expected to be retained in the excited  $^1B_2$  state, where both the  $\text{N}-\text{N}$  bond length and the  $\text{N}-\text{C}-\text{N}$  angle are strongly increased compared to those of the ground state. The long  $\text{N}-\text{N}$  bond and the widened  $\text{N}-\text{C}-\text{N}$  angle in the excited  $^1B_2$  state facilitate a rearrangement of **V** through  $\text{N}=\text{N}$  bond cleavage. In fact, the transition state for the rearrangement of **V** to the open-chain isomer ONCN (**I**) at the ground-state surface features a widened  $\text{N}-\text{C}-\text{N}$  angle of  $103^\circ$ .<sup>[1c]</sup>

## Conclusions

Diazirine (**V**) obtained from low-pressure flash-pyrolysis of  $\text{OC}(\text{N}_3)_2$  has been purified by fractional condensation. The decomposition of gaseous **V** was found to be sensitive to surface catalysis, since its half-life increased from minutes in stainless steel containers, to about 1.4 h in glass cells (first-order kinetics),<sup>[10]</sup> to more than 30 h (second-order kinetics) in a carefully dried quartz cell. The IR and Raman spectra of the solid as well as the UV/Vis spectrum of the gas have been recorded and analyzed. An intriguing feature is the distinctive change of its spectral properties from the gas to solid state, which probably can be attributed to strong intermolecular interactions involving the nitrogen lone pairs. Most obvious is the change in color by cooling the violet gas to a brownish-yellow solid, suggesting an electronic stabilization of the HOMO in the solid state.

The photochemistry of **V** was studied in solid Ar matrices by using visible light ( $\lambda > 520$  nm) and ArF excimer laser ( $\lambda = 193$  nm) irradiation. While visible light induced decomposition into  $\text{N}_2$  and CO, isomerization to the open-chain isomers NOCN, ONNC, and ONCN was observed upon ArF excimer laser photolysis. The different photodecomposition pathways are consistent with ab initio calculations.

## Experimental Section

**Caution!** Carbonyl diazide,  $\text{OC}(\text{N}_3)_2$ , is an extremely explosive and shock-sensitive compound in the liquid and solid states. Safety precautions must be taken, including face shields, leather gloves, and protective leather clothing.

Fluorocarbonyl azide,  $\text{FC}(\text{O})\text{N}_3$ , was prepared according to a reported procedure<sup>[24]</sup> with minor modifications concerning the reaction vessel. Instead of small flame-sealed ampoules, tube-like glass vessels were used (volume 25 mL, length 20 cm), which were equipped with a valve fitted with a PTFE stem (Young, London, UK). The use of such reaction vessels avoids the hazard of explosions arising from cutting flame-sealed ampoules containing explosive azides.

Carbonyl diazide,  $\text{OC}(\text{N}_3)_2$ , was synthesized from  $\text{FC}(\text{O})\text{N}_3$  and  $\text{NaN}_3$ . Gaseous  $\text{FC}(\text{O})\text{N}_3$  (0.46 mmol) was condensed into the reaction vessel, which was charged with dried  $\text{NaN}_3$  (30 mg, 0.46 mmol) and kept at  $-196^\circ\text{C}$ . The vessel was slowly warmed to room temperature and kept for 2 d. The vessel was then very slowly opened to the vacuum line, and the volatile products were directed through three cold traps kept at  $-60$ ,  $-100$ , and  $-196^\circ\text{C}$ .  $\text{OC}(\text{N}_3)_2$  (ca. 50 mg) was retained in the first trap as a white solid, and its purity was checked by gas-phase IR spectroscopy.<sup>[14]</sup> Traces of  $\text{FC}(\text{O})\text{N}_3$  were observed in the middle trap, and traces of  $\text{SiF}_4$  were found in the last trap.

The preparation of diazirine was performed by low-pressure flash pyrolysis of  $\text{OC}(\text{N}_3)_2$  as described in the literature.<sup>[10]</sup> However, instead of a glass furnace, a heated quartz tube with some quartz wool inside was used. In a typical experiment, the quartz container charged with ca. 60 mg of  $\text{OC}(\text{N}_3)_2$  was immersed in an ice/salt bath ( $-15^\circ\text{C}$ ). The slowly sublimed sample passed through the quartz tube (14 mm o.d., 6 mm i.d., heated zone 40 mm long) and heated to  $420^\circ\text{C}$ . The pyrolysis products were collected in two

U-traps kept at  $-110$  and  $-196$  °C. Some undecomposed diazide was trapped in the first trap, and a pale yellow solid was obtained in the second trap. After two batches, the products collected in the  $-196$  °C trap were separated by passing through three cold traps kept at  $-110$ ,  $-145$ , and  $-196$  °C. Cyclic  $N_2CO$  was retained in the middle trap as a brownish-yellow solid, and traces of HNC $O$  were found in the trap at  $-196$  °C.

Low-temperature Raman measurements were performed on solid samples, which were condensed onto a stainless steel finger cooled to 77 K in a high vacuum. The spectra were recorded with a Bruker-Equinox 55 FRA 106/S FT-Raman spectrometer by using a 1064 nm Nd:YAG laser (200 mW), and 500 scans were averaged for each spectrum at a resolution of  $2\text{ cm}^{-1}$ . UV/Vis spectra were measured in a closed quartz cell (50 mm long, 20 mm diameter) with a Perkin-Elmer Lambda 900 UV spectrometer by using a data point distance of 0.5 nm and an integration time of 2 s.

Infrared spectra of matrix-isolated diazirinone were recorded with an FTIR spectrometer (IFS 66v/S Bruker) in a reflectance mode by using a transfer optic. A KBr beam splitter and an MCT detector were used in the region of  $5000\text{--}530\text{ cm}^{-1}$ . For each spectrum 200 scans at a resolution of  $0.25\text{ cm}^{-1}$  were coadded. The matrix was prepared by passing argon gas through a cold glass U-trap ( $-140$  °C) containing ca. 1 mg of  $N_2CO$ . At a flow rate of  $2\text{ mmol h}^{-1}$  of Ar (Ne), the resulting mixture ( $N_2CO$ /inert gas  $\approx 1:1000$ , estimated) was deposited onto the cryogenic matrix support (Rh plated Cu block, 16 K for Ar and 6 K for Ne). Low-temperature IR spectra of solid  $N_2CO$  were recorded at 6 K by slowly depositing the vapor of the solid kept at  $-140$  °C onto a thin film of Ne covering the matrix support. Details of the matrix apparatus have been described elsewhere.<sup>[25]</sup> Photolysis experiments were carried out by using an ArF excimer laser (Lambda-Physik), as well as a medium-pressure mercury arc lamp (TQ 150, Heraeus), equipped with a water-cooled quartz lens and various cutoff filters (Schott).

### Computational Details

The  $A^1B_1$  excited state of V was studied with the equation-of-motion coupled-cluster (EOM-CC) approach<sup>[26]</sup> by using two different atomic natural orbital basis sets. These are designated as ANO0 and ANO1, and were described in our previous publication on this molecule.<sup>[10]</sup> By using these basis sets, both the EOM-CCSD and EOM-CCSDT approaches were used to find the equilibrium geometry and harmonic force constants of the excited state, while the CCSD<sup>[27]</sup> and CCSD(T)<sup>[28]</sup> approximations were used for the ground state. Term energies  $T_0$  were obtained by subtracting the ground-state energy at the corresponding equilibrium geometry obtained in the same basis and with the CCSD method (for EOM-CCSD term energies) or CCSD(T) (for EOM-CCSDT) term energies. A zero-point correction was included, as calculated from the harmonic frequencies. All calculations were done in the frozen-core approximation and with the CFOUR<sup>[29]</sup> program package.

**Supporting Information** (see footnote on the first page of this article): Kinetic plots of the decomposition of diazirinone, UV/Vis spectra of  $N_2CO$ , IR difference spectra of Ar-matrix-isolated  $N_2CO$ , IR frequencies and frontier molecular orbitals of diazirinone, and vibrational assignments for the visible transition of  $N_2CO$ .

### Acknowledgments

This work was supported by the Deutsche Forschungsgemeinschaft (DFG) (WI 663/26-1, BE 4415/1-1) and the United States National

Science Foundation. We are indebted to T. Benter and his group to make use of the ArF laser.

- [1] a) A. A. Korkin, P. von R. Schleyer, R. J. Boyd, *Chem. Phys. Lett.* **1994**, *227*, 312–320; b) A. A. Korkin, A. Balkova, R. J. Bartlett, R. J. Boyd, P. von R. Schleyer, *J. Phys. Chem.* **1996**, *100*, 5702–5714; c) R. S. Zhu, M. C. Lin, *J. Phys. Chem. A* **2007**, *111*, 6766–6771; d) D. Toffoli, M. Sparta, O. Christiansen, *Mol. Phys.* **2011**, *109*, 673–685.
- [2] F. Cacace, G. de Petris, A. Troiani, *Science* **2002**, *295*, 480–481, and references therein.
- [3] D. Schröder, C. Heinemann, H. Schwarz, J. N. Harvey, S. Dua, S. J. Blanksby, J. H. Bowie, *Chem. Eur. J.* **1998**, *4*, 2550–2557, and references therein.
- [4] See, for example: a) P. Horsewood, G. W. Kirby, *J. Chem. Soc., Chem. Commun.* **1971**, 1139–1140; b) R. Dickinson, G. W. Kirby, J. G. Sweeny, J. K. Tyler, *J. Chem. Soc., Chem. Commun.* **1973**, 241–242; c) E. A. Dorko, L. Buelow, *J. Chem. Phys.* **1975**, *62*, 1869–1872.
- [5] G. Maier, H. P. Reisenauer, J. Eckwert, M. Naumann, M. D. Marco, *Angew. Chem.* **1997**, *109*, 1785–1787; *Angew. Chem. Int. Ed. Engl.* **1997**, *36*, 1707–1709.
- [6] G. de Petris, F. Cacace, R. Cipollini, A. Cartoni, M. Rosi, *Angew. Chem.* **2005**, *117*, 466–469; *Angew. Chem. Int. Ed.* **2005**, *44*, 462–465.
- [7] a) R. A. Moss, L. Wang, K. Krogh-Jespersen, *J. Am. Chem. Soc.* **2009**, *131*, 2128–2130; b) R. A. Moss, *Pure Appl. Chem.* **2007**, *79*, 993–1001; c) R. A. Moss, *Acc. Chem. Res.* **2006**, *39*, 267–272; d) G. Chu, R. A. Moss, R. R. Sauer, *J. Am. Chem. Soc.* **2005**, *127*, 14206–14207.
- [8] R. A. Moss, G. Chu, R. R. Sauer, *J. Am. Chem. Soc.* **2005**, *127*, 2408–2409.
- [9] a) C. J. Shaffer, B. J. Esselman, R. J. McMahon, J. F. Stanton, R. C. Woods, *J. Org. Chem.* **2010**, *75*, 1815–1821; b) R. A. Moss, R. R. Sauer, *Tetrahedron Lett.* **2010**, *51*, 3266–3268; c) R. A. Moss, *J. Org. Chem.* **2010**, *75*, 5773–5783.
- [10] X. Q. Zeng, H. Beckers, H. Willner, J. F. Stanton, *Angew. Chem.* **2011**, *123*, 1758–1761; *Angew. Chem. Int. Ed.* **2011**, *50*, 1720–1723.
- [11] A. Perrin, X. Q. Zeng, H. Beckers, H. Willner, *J. Mol. Spectrosc.* **2011**, *269*, 30–35.
- [12] Y. S. Kim, F. Zhang, R. I. Kaiser, *Phys. Chem. Chem. Phys.* **2011**, *13*, 15766–15773.
- [13] C. J. Shaffer, D. Schröder, *Angew. Chem.* **2011**, *123*, 2729–2730; *Angew. Chem. Int. Ed.* **2011**, *50*, 2677–2678.
- [14] X. Q. Zeng, M. Gerken, H. Beckers, H. Willner, *Inorg. Chem.* **2010**, *49*, 9694–9699.
- [15] W. Gombler, H. Willner, *J. Phys. E.: Sci. Instrum.* **1987**, *20*, 1286.
- [16] J. Weidlein, U. Müller, K. Dehnicke, *Schwingungsspektroskopie*, Thieme, Stuttgart, Germany, **1982**, p. 37.
- [17] P. H. Hepburn, J. M. Hollas, *J. Mol. Spectrosc.* **1974**, *50*, 126–141.
- [18] L. C. Robertson, J. A. Merritt, *J. Mol. Spectrosc.* **1966**, *19*, 372–388.
- [19] a) D.-S. Ahn, S.-Y. Kim, G.-I. Lim, S. Lee, Y. S. Choi, S. K. Kim, *Angew. Chem.* **2010**, *122*, 1266–1269; *Angew. Chem. Int. Ed.* **2010**, *49*, 1244–1247; b) I. Fedorov, L. Koziol, A. K. Mollner, A. I. Krylov, H. Reisler, *J. Phys. Chem. A* **2009**, *113*, 7412–7421.
- [20] P. Pyykkö, M. Atsumi, *Chem. Eur. J.* **2009**, *15*, 12770–12779.
- [21] U. P. Verma, K. Möller, J. Vogt, M. Winnewisser, J. J. Christiansen, *Can. J. Phys.* **1985**, *63*, 1173–1183.
- [22] J. L. Hencher, S. H. Bauer, *J. Am. Chem. Soc.* **1967**, *89*, 5527–5531.
- [23] H. A. Bent, *Chem. Rev.* **1961**, *61*, 275–311.
- [24] J. Jacobs, B. Jülicher, G. Schatte, H. Willner, H.-G. Mack, *Chem. Ber.* **1993**, *126*, 2167–2176.

- [25] H. G. Schnöckel, H. Willner, in *Infrared and Raman Spectroscopy, Methods and Applications* (Ed.: B. Schrader), VCH, Weinheim, **1994**.
- [26] J. F. Stanton, R. J. Bartlett, *J. Chem. Phys.* **1993**, *98*, 7029–7039.
- [27] G. D. Purvis, R. J. Bartlett, *J. Chem. Phys.* **1982**, *76*, 1910–1918.
- [28] K. Raghavachari, G. W. Trucks, J. A. Pople, M. Head-Gordon, *Chem. Phys. Lett.* **1989**, *157*, 479–483.
- [29] J. F. Stanton, J. Gauss, M. E. Harding, P. G. Szalay, A. A. Auer, R. J. Bartlett, U. Benedikt, C. Berger, D. E. Bernholdt, Y. J. Bomble, L. Cheng, O. Christiansen, M. Heckert, O. Heun, C. Huber, T.-C. Jagau, D. Jonsson, J. Jusélius, K. Klein, W. J. Lauderdale, D. A. Matthews, T. Metzroth, L. A. Mück, D. P. O'Neill, D. R. Price, E. Prochnow, C. Puzzarini, K. Ruud, F. Schiffmann, W. Schwalbach, S. Stopkowitz, A. Tajti, J. Vázquez, F. Wang, J. D. Watts, J. Almlöf, P. R. Taylor, T. Helgaker, H. J. A. Jensen, P. Jørgensen, J. Olsen, A. V. Mitin, C. van Wüllen, *CFOUR, Coupled-Cluster techniques for Computational Chemistry, a quantum-chemical program package*, **2010**, <http://www.cfour.de>.

Received: April 4, 2012  
Published Online: June 15, 2012